Experimental study on machining deformation of large scale slender beam with weak stiffness of Ti6Al4V

Qimeng Liu
Changchun University of Science and Technology
Jinkai Xu
Changchun University of Science and Technology
Huadong Yu (172024452@qq.com)
Changchun University of Science and Technology

Research Article

Keywords: Large scale slender beam, Deformation, Auxiliary support, Titanium Alloy

Posted Date: March 24th, 2021

DOI: https://doi.org/10.21203/rs.3.rs-339491/v1

Version of Record: A version of this preprint was published at The International Journal of Advanced Manufacturing Technology on July 6th, 2021. See the published version at https://doi.org/10.1007/s00170-021-07586-2.

ORIGINAL ARTICLE

Experimental study on machining deformation of large scale slender beam with weak stiffness of Ti6Al4V

Qimeng Liu[1],

Jinkai Xu[1],

Huadong Yu[1*]172024452@qq.com

[1-]Ministry of Education Key Laboratory for Cross-Scale Micro and Nano Manufacturing

Changchun University of Science and Technology

Changchun 130022, China

Abstract

Large-scale slender beam structures with weak stiffness are widely used in the aviation field. There will be a great deformation problem in machining because the overall stiffness of slender beam parts is lower. Firstly, the cutting mechanism and stability theory of the Ti6Al4V material are analyzed, and then the auxiliary support is carried out according to the machining characteristics of the slender beam structure. The feasibility of the deformation suppression measures for the slender beam is verified by experiments. The experimental analysis shows that on the basis of fulcrum auxiliary support, the filling of paraffin melt material is capable of increasing the damping of the whole system, improving the overall stiffness of the machining system, and inhibiting the chatter effect of machining. This method is effective to greatly improve the accuracy and efficiency during machining of slender beam parts. On the premise of the method of processing support with the combination of fulcrum and paraffin, if the tool wear is effectively controlled, the high precision machining of large-scale slender beams can be realized effectively, and the machining deformation of slender beams can be reduced. Although high speed milling has excellent machining effect on the machining accuracy of titanium alloy materials, severe tool wear is observed during high-speed milling of titanium alloy materials. Therefore, high-speed milling of titanium alloy slender beam is suitable to be carried out in the finishing process, which can effectively control tool wear and improve the machining accuracy of parts. Finally, the process verification of typical weak stiffness slender beam skeleton parts is carried out. Through the theoretical and technical support of the experimental scheme, the machining of large-scale slender beam structure parts with weak stiffness is realized.

Keywords

Large scale slender beam

Deformation

Auxiliary support

Titanium Alloy

1 Introduction

Titanium alloy is one of the main materials of the whole structure of aviation. With the development of aviation technology in recent years, the application of titanium alloy materials in high maneuvering aircraft has been widely popularized, especially Ti6Al4V. It is a heat-resistant alloy, its elastic modulus is 70.3 GPa, the compression modulus is 73.8 GPa, the density is 4.44 g/cm3, the Poisson's ratio is 0.33, and the melting point range is 1560~1680℃. Its chemical composition is shown in Table 1.

Table 1 Chemical composition of Ti6Al4V

Composition	Al	V	Fe	Si	O	C	N	H	其他	Ti
Content(%)	5.5~6.5	3.5~4.5	0.25	0.15	0.13	0.08	0.05	0.012	0.5	其余

Ti6Al4V material is mainly used to make mechanical structure of aviation products, such as frame, impeller, wing plate and beam structure. However, there are still some technical problems in the application of titanium alloy materials for processing of large-scale slender beam structure at home and abroad and, for example, serious deformation is the most common problem encountered during machining [1-2]. Although the design of slender beam structure has many advantages, when the workpiece is removed from the fixture, deformation such as bending, twisting, or combined bending and torsion often occurs during machining due to its large aspect ratio, high material removal rate and poor rigidity, which makes it difficult for the parts to meet the design requirements.

The Nervi S of the United States established a mathematical prediction model of machining deformation caused by initial residual stress of blank, and studied the relationship [3] between structural deformation and the distribution state of initial blank stress [3]. Keith studied the influence of residual stress on machining deformation. Results indicated that the machining stress was closely related to the radius of arc tip and the radius of blunt circle of cutting edge. For aeronautical thin-walled structure, the machining residual stress had a certain effect on the machining deformation of workpiece [4]. By using the neural network theory, Ratchev and others established the flexible prediction model of the milling deformation of thin-walled parts, and then established the prediction model of the machining error of the thin-walled workpiece by combining it with the finite element analysis method [5-7]. Tlusty proposed the effective use of unprocessed parts as support, and explored the method of milling path optimization using the overall rigidity of aeronautical structural parts[8]. Hiroyasu studied the deformation of thin-walled parts caused by cutting force, and designed the parallel double spindle machining method[9].

Domestic scholars have focused on the deformation problem occurred during machining of aeronautical integral structural parts since 2000 and have conducted studies by performing tests, mechanical modeling and finite element analysis. Dr. Huang Yunlin from Nanjing University of Science and Technology identified suitable cutting parameters using stable leaf flap simulation for the rough and finish machining of housing cavity, and verified the technical effectiveness of machining of

thin-walled parts for the whole impeller from the aspects of blank and tool selection, fixture design, machining process flow of integral impeller, NC program compilation and simulation, specimen processing and measurement, ensuring feasible mass milling of thin-walled parts with high efficiency, high quality and low cost [10]. Dr. Wang Ming from Harbin University of Technology selected the cutting parameters of stable point by MATLAB simulation. The results showed that the stability analysis method made the reasonable selection of cutting parameters possible which could avoid the occurrence of chatter, thus improving the machining quality and efficiency of thin-walled parts[11]. Dong Guojun, Harbin University of Technology, has carried out molecular dynamics simulation and experimental research on tool wear mechanism, and studied tool wear mechanism according to the change of chemical composition of tool tip, which provides technical support for cutting tool wear[12].

Although many scholars at home and abroad have done a lot of academic research in thin walls with weak stiffness, impellers and frame parts, there is little research on the machining deformation of slender beam parts with large scale aspect ratio, and a breakthrough is needed in this direction. Processing a slender beam structure becomes difficult because it will be in the cantilever state and deformation and chatter will occur during machining. Therefore, the paper takes the slender beam structure with weak stiffness as a research object and studies a method to suppress the deformation occurred during processing. In addition, experiments are performed to further study the deformation behavior of a cantilever structure with weak stiffness during processing by considering the properties of Ti6Al4V. The clamping method of the slender beam structure is studied to improve the overall machining stiffness and damping to make it stable. Based on the optimal clamping mode, the influence of different tool wear and milling parameters on the machining deformation of weak stiffness slender beam is explored, which provides technical support for the machining technology and clamping method of typical slender beam parts with weak stiffness.

2 Theoretical Analysis of Cutting Mechanism and Milling Stability of Ti6Al4V

2.1 Cutting Mechanism Analysis

The chip formation process of metal machining is actually the deformation process of material cutting layer. The chip separation process can be roughly divided into the first deformation zone (shear slip), the second deformation zone (fibrosis), and the third deformation zone (fibrosis and work hardening). As shown in fig.1a, the first deformation zone interacts with the second deformation zone. When the friction force of the knife surface is large, the chip discharge is not smooth, the extrusion deformation intensifies, and the shear slip deformation in the first deformation zone increases. In the contact area between the machined surface and the rear tool surface, due to the extrusion friction between the tool edge circle and the rear tool surface, the machined surface is fibrosis and work hardening, thus forming the third deformation zone[1].

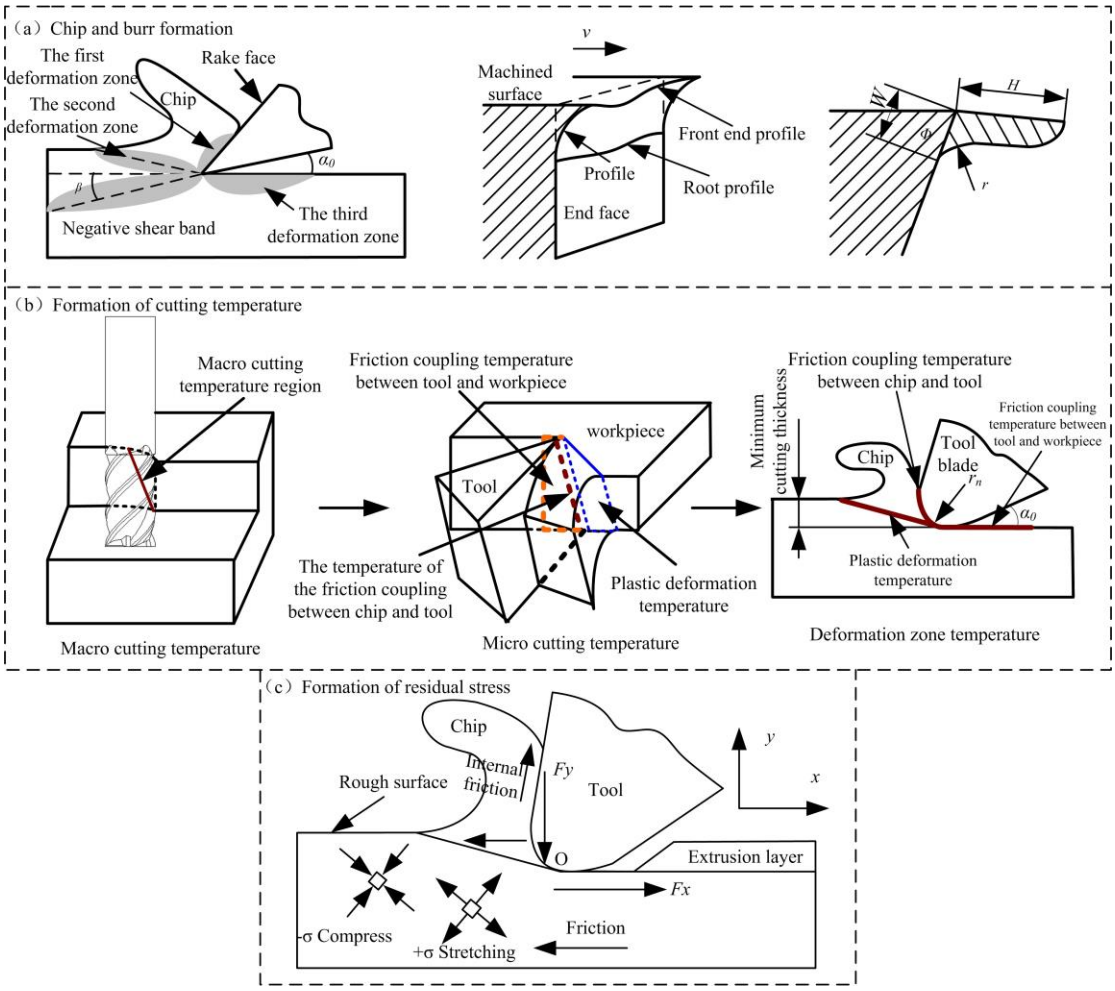

Fig. 1 Principle of Metal Cutting

Burr is a part of the edge area of the workpiece, which is a part of the chip removal in theory. It is a part of the machining process. The definition of burr parameters is an important standard for burr study and evaluating the energy consumption of deburring. The basic parameters of burr are usually studied by arbitrary cross section of burr. The main parameters of burr are height, root thickness and root radius. As shown in fig.1a, burr height H refers to the maximum distance between the ideal end face of the workpiece terminal surface measured on the cross section and the profile of the burr cross section. Burr root thickness W refers to the distance from the plastic deformation convex starting point to the ideal surface of the workpiece measured on the end surface of the workpiece. The radius of the burr root circle is the radius of curvature of the root geometric curve of the burr cross section measured on the cross section. Obviously, the size of burr height H directly affects the dimensional accuracy and shape accuracy of the workpiece, while the thickness of burr root W has a relation to the efforts of deburring. By using characteristic parameters H and W, the specific size and shape of burr cross section can be expressed[13].

The cutting temperature produced by the milling cutter in the machining process can simplify the three-dimensional cutting into a simple two-dimensional plane oblique angle cutting, that is, the milling cutter can be separated into countless units along the spiral cutting line. The cutting process of a single

unit is simplified diagonal cutting. Figure 1b is a simplified diagram of milling temperature model. The milling temperature is mainly from three regions: (1) The cutting temperature region of the front cutter surface caused by friction between the chip and the front cutter surface; (2) The cutting temperature region of the rear cutter surface produced by the friction between the rear cutter surface and the workpiece and (3) Temperature region of plastic deformation of shear surface produced by shear slip of metal plastic deformation[14].

As shown in Fig. 1c, the action of the arc radius of the tool resulted in a triangular region where tensile stress and extrusion stress combined on the workpiece when cutting. The grains in this region were elongated along the Y-axis due to stretching, and plastic shortened along the X-axis because of compression, finally forming a residual tensile stress under the action of these two behaviors. Consequently, the third deformation zone was formed in the workpiece, and the friction force Fx and normal force Fy acted on the surface layer of the workpiece. The normal force caused plastic deformation on the surface layer in the direction of Y-axis while the friction force Fx induced the surface layer to produce plastic deformation along the X-axis direction, which led to residual compressive stress on the machined surface[15].

2.2 Dynamic Milling Force Model

The mathematical model of dynamic milling stability is the basis for the study of machining process stability and dynamic machining error. The difficulty of dynamic milling stability modeling lies in the modeling of cutting thickness. As shown in Fig. 2, the milling system can be simplified into two "spring-damping" systems with vertical degrees of freedom.

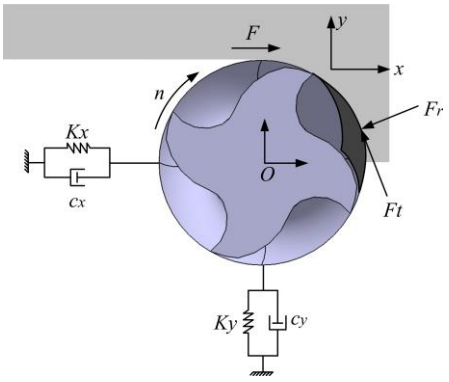

Fig. 2 Milling Vibration Systems

The milling dynamics equation can be expressed as a differential equation

$$\begin{cases} m_x \ddot{x} + c_x \dot{x} + k_x x = \sum_{j=1}^{N} F_{xj} = F_x(t) \\ m_y \ddot{y} + c_y \dot{y} + k_y y = \sum_{j=1}^{N} F_{yj} = F_y(t) \end{cases} \tag{1}$$

where m_x、m_y — Quality of milling system in X, Y direction(kg);

c_x， c_y — Damping of milling system in X, Y directions(Ns/m);

k_x， k_y — Stiffness of milling system in X, Y direction(N/m) ;

F_{xj}， F_{yj} — Cutting force component (N) in X and Y direction acting on cutter teeth *j*.

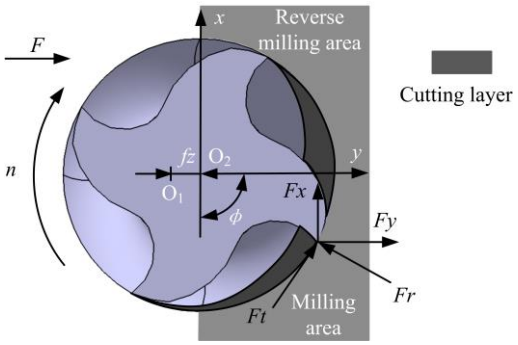

Fig. 3 Force distribution of milling cutter

Figure 3 shows the force distribution of milling cutter blade, in which the *Ft* is tangential cutting force and the *Fr* is radial cutting force. In the milling process, the machining system is excited by the milling force in the *X* and *Y* directions, resulting in the corresponding dynamic displacement *x* and *y*. Coordinate transformation of dynamic displacement in cutting thickness direction of cutter teeth v_j=-*x*sinφ_j-*y*cosφ_j. As the two-dimensional static cutting thickness has nothing to do with the mechanism of regenerative chatter, it can be ignored in the flutter stability analysis. So the two-dimensional dynamic cutting thickness can be expressed in the following formula[10].

$$h_j(\phi) = (x - x_0)\sin\Omega t + (y - y_0)\cos\Omega t \tag{2}$$

where (*x*, *y*) represents the dynamic displacement of the current tool tooth period, and (x_0, y_0) represents the dynamic displacement of the former tool tooth period. The rotation angular velocity of the spindle is Ω(*rad*/*s*). Then the radial contact angle φ_j is transformed into Ωt with time. φ_j=(*j*-1)φ_p+φ is the instantaneous radial contact angle of cutter tooth *j*. Since the number of cutting edges *j* is 4, the cutting angles of the four cutting edges are：$\varphi_0 = \varphi$， φ_1=φ+π/2， φ_2=φ+π， φ_3=φ+3π/2。

The tangential cutting force F_{tj} and the radial cutting force F_{rj} of acting on the cutter tooth *j* are[10]

$$\begin{aligned} F_{tj} &= K_t a_p h(\phi_j) \\ F_{rj} &= K_r F_{tj} \end{aligned} \tag{3}$$

where a_p is axial tangential depth(mm); K_t， K_r—tangential and radial cutting force coefficients, respectively(*N*/*m*).

The total cutting force acting on the tool is

$$F_x = \sum_{j=0}^{N_f-1} F_{xj}(\psi_j); \quad F_y = \sum_{j=0}^{N_f-1} F_{yj}(\psi_j) \tag{4}$$

Finally, we substitute formula (2) and (3) into formula (4) and express them in the form of matrix

$$\begin{Bmatrix} Fx \\ Fy \end{Bmatrix} = \frac{1}{2} a_p K_t [\mathrm{A}] \begin{Bmatrix} \Delta x \\ \Delta y \end{Bmatrix} \tag{5}$$

where $\triangle x=x-x_0$, $\triangle y=y-y_0$, $[A] = \begin{bmatrix} \alpha_{xx} & \alpha_{xy} \\ \alpha_{yx} & \alpha_{yy} \end{bmatrix}$

$$\alpha_{xx} = \sum_{j=0}^{N-1} g_j \left[-\sin 2\phi_j - K_r (1 - \cos 2\phi_j) \right] \quad ; \alpha_{xy} = \sum_{j=0}^{N-1} g_j \left[-(1 + \cos 2\phi_j) - K_r \sin 2\phi_j \right]$$

$$\alpha_{yx} = \sum_{j=0}^{N-1} g_j \left[(1 - \cos 2\phi_j) + K_r \sin 2\phi_j \right] \quad ; \alpha_{yy} = \sum_{j=0}^{N_f-1} g_j \left[\sin 2\phi_j - K_r (1 + \cos 2\phi_j) \right]$$

Considering the variation of these parameters with time and angular velocity, equation (6) is expressed in matrix form in time domain as follows

$$\{F_t\} = \frac{1}{2} a_p K_t [A(t)] \{\Delta(t)\} \tag{6}$$

where $A(t)$ is a periodic function of $\omega=N\Omega$ and $T=2\pi/\omega$. The expansion form of Fourier series is

$$[A(t)] = \sum_{r=-\infty}^{\infty} [A_r] e^{ir\omega t}; [A_r] = \frac{1}{T} \int_0^T [A(t)] e^{-ir\omega t} dt \tag{7}$$

Ignore the influence of higher harmonics and retain the DC component $A(0)$

$$[A(0)] = \frac{1}{\phi_p} \int_{\phi st}^{\phi ex} [A(\phi)] d\phi = \frac{N}{2\pi} [\mathrm{A}] \tag{8}$$

where $[A] = \begin{bmatrix} \alpha_{xx} & \alpha_{xy} \\ \alpha_{yx} & \alpha_{yy} \end{bmatrix}$

By substituting equation (8) into equation (6), the expression of dynamic milling force coefficient can be simplified as

$$\{F(t)\} = \frac{1}{2} a_p K_t [A_0] \{\Delta(t)\} \tag{9}$$

2.3 Flutter stability limit

As shown in Fig. 2, a tool-workpiece system can be simplified to X and Y two-degree-of-freedom vibration systems in two vertical directions [13]. Let the frequency response function of the tool workpiece system be

$$[G(i\omega)] = \begin{bmatrix} G_{xx}(i\omega) & G_{xy}(i\omega) \\ G_{yx}(i\omega) & G_{yy}(i\omega) \end{bmatrix} \tag{10}$$

Where $G_{xx}(i\omega)$ and $G_{yy}(i\omega)$ represent the direct frequency response functions of the tool workpiece system in X and Y directions respectively. $G_{xy}(i\omega)$ and $G_{yx}(i\omega)$ represent the cross frequency response functions of the tool workpiece system in X and Y directions respectively. Let the relative vibration vectors of the tool and the workpiece at the current time (t) and the previous cutting time (t -T) be

$$\begin{aligned}\{r\} &= \{x(t)\, y(t)\}^T \\ \{r_0\} &= \{x(t-T)\, y(t-T)\}^T\end{aligned} \tag{11}$$

The frequency domain of the relative vibration function of the tool and workpiece at the current time and the cutting time of the previous cutter tooth at flutter frequency ω_c is expressed as[16]

$$\begin{aligned}\{r(i\omega_c)\} &= [G(i\omega_c)]\{F\}e^{i\omega_c t} \\ \{r_0(i\omega_c)\} &= e^{i\omega_c t}\{r(i\omega_c)\}\end{aligned} \tag{12}$$

Regenerative displacement

$$\{\Delta(i\omega_c)\} = \{r(i\omega_c)\} - \{r_0(i\omega_c)\} = [1 - e^{-i\omega_c tT}]e^{i\omega_c tT}[G(i\omega_c)]\{F\} \tag{13}$$

Let the determinant be zero, find the special solution of the equation, and the characteristic equation of the tool workpiece closed-loop dynamic system is

$$\det\{[I] - \frac{1}{2}a_p K_{IC}(1 - e^{-i\omega_c T})[A_0][G_0(i\omega_c)]\} = 0 \tag{14}$$

The characteristic equations obtained by further simplification are as follows

$$\det\{[I] + \Lambda[G_0(i\omega_c)]\} = 0 \tag{15}$$

The eigenvalues can be obtained by neglecting the influence of the cross functions G_{xy} and G_{yx}: $\Lambda = -\frac{1}{2a_0}(a_1 \pm \sqrt{a_1^2 - 4a_0})$, among: $a_0 = G_{xx}(i\omega_c)G_{yy}(i\omega_c)(\alpha_{xx}\alpha_{yy} - \alpha_{xy}\alpha_{yx})$, $a_1 = \alpha_{xx}G_{xx}(i\omega_c) + \alpha_{yy}G_{yy}(i\omega_c)$。

Its eigenvalues contain real and imaginary parts because the transfer function is plural. As the axial cutting depth is real number, by substituting $\Lambda = \Lambda_R + i\Lambda_I$ and $e^{-i\omega cT} = \cos(\omega_c T) - i\sin(\omega_c T)$ into eigenvalues, the ultimate axial tangential depth at flutter frequency can be obtained[17]:

$$a_{p\lim} = -\frac{2\pi}{NK_{tc}}\{\frac{\Lambda_R(1-\cos\omega_c T) + \Lambda_I \sin\omega_c T + i[\Lambda_I(1-\cos\omega_c T) + \Lambda_R \sin\omega_c T]}{1-\cos\omega_c T}\} \tag{16}$$

The upper imaginary part is zero because the axial cutting depth a_p is a real number, and the final expression of ultimate axial depth can be simplified

$$a_{p\lim} = -\frac{2\pi\Lambda_R(1+\kappa^2)}{NK_{tc}} \tag{17}$$

It can be seen that if the flutter frequency ω_c is given, the limit axial cutting depth can be obtained according to the above formula, and

$$\kappa = \tan\psi = \tan[\frac{\pi}{2} - \frac{\omega_c T}{2}] \tag{18}$$

Where $\Psi = \arctan\kappa$ is the phase shift of eigenvalue. $\varepsilon = \pi - 2\Psi$ is the phase shift between internal and external modulation. Therefore, if the vibration ripple left by the cutting arc is an integer k, $\omega_c T = \varepsilon + 2k\pi$. The spindle speed can be obtained by calculating the cutting cycle T

$$n = \frac{60}{N[(2k+1)\pi - 2\tan^{-1}(\Lambda_I / \Lambda_R)]} \tag{19}$$

It can be concluded that in order to improve the cutting stability, the high precision parts can be processed by increasing the damping and the overall stiffness of the machining system as well as reducing the cutting force.

3 Deformation control measures and processing experiment of slender beam

3.1 Influencing factors and restraining methods of processing deformation of slender beam with weak stiffness

For the deformation problems of weak stiffness parts, the influencing factors of deformation in the processing of suspension beam parts with weak rigidity need to be investigated first, as shown in Fig. 4. It is found that the problems of low stiffness and deformation can be effectively solved by increasing the overall machining stiffness of weak stiffness parts and the damping of the system. At the same time, tool wear and machined surface stress can be improved.

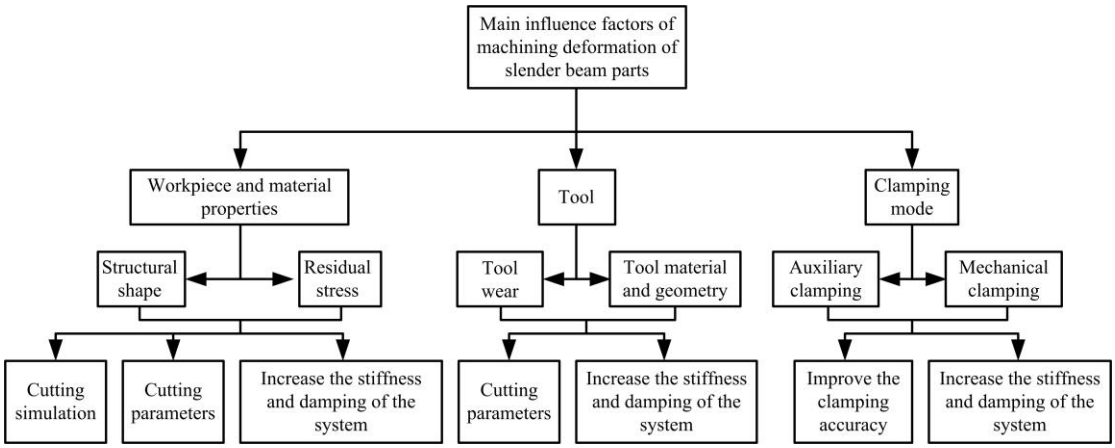

Fig. 4 Factors influencing deformation of slender beam parts with weak stiffness

The clamping mode of weak stiffness parts is the most important factor that directly influence the machining accuracy of such parts. When clamping slender beam parts with weak stiffness, pressure plate clamping is not recommended because the special suspension state of the parts will cause the parts to be subjected to cutting force during the machining process, and hence the suspension deformation will occur because of the weak stiffness. Upon unloading, even if the condition of the parts after machining is satisfied, the machined parts will suffer deformation due to the release of the external clamping force. Therefore, it is necessary to ensure the overall processing stiffness of the parts during processing, so that it not only can enable the stable clamping of the parts, but also improve the stiffness of the overall workpiece processing system. To achieve this, the auxiliary support is necessary for the cantilever parts aiming to inhibit the chattering or deformation phenomenon occurs during

machining. On the other hand, paraffin filling is carried out on the basis of auxiliary support to indirectly increase the damping of the workpiece processing system, which is capable of further improving the machining accuracy. The filling of paraffin melt can make it possible to suppress chatter in the process of machining, thereby greatly improving process efficiency. Figure 5 shows the effect of deformation with or without auxiliary support.

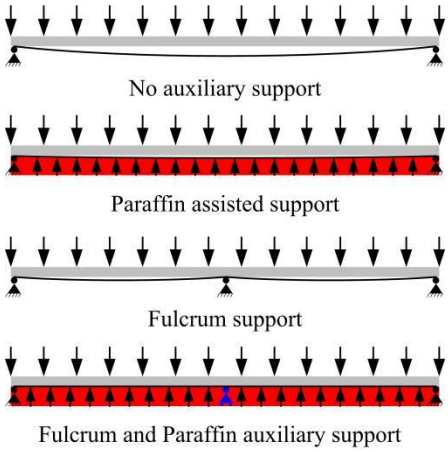

Fig. 5 Schematic illustration of deformation effect of auxiliary support

3.2 Experimental scheme of deformation of slender beam with weak stiffness

In this experiment, the clamping methods of the slender beam are designed with no auxiliary support, fulcrum auxiliary support, paraffin auxiliary support, and fulcrum + paraffin auxiliary support. The number of fulcrum is divided and increased according to the length of suspension beam. The processing deformation scheme of slender beam with weak stiffness is shown in Table 2. The experimental environment is shown in Figure 6.

Table 2 Experimental conditions

No.	Name	
1	NC Machining Center	Tool type: 6mm diameter, 4 edges, 45 ° helix angle. The surface is coated with TiSiN cemented carbide end mill. The clamping suspension is 30mm.
2	Paraffin wax	
3	3D edge seeker（The accuracy is 0.002mm）	
4	Micrometer	
5	Size of titanium alloy blank	Length 440mm×width 12mm×height 12mm
6	Dimension of slender beam structure of weak rigidity after machining	Length 420mm×width 8.6mm×height 8.6mm
7	Processing cooling mode	Cutting fluid assisted cutting
8	Residual stress measuring instrument	Measuring angle： 0°，±15°，±45°，±60°
9	Processing support of slender beam of weak stiffness	No auxiliary support
10		Fulcrum support

11			Paraffin assisted support
12			Fulcrum+Paraffin auxiliary support
13	On the basis of the above	Spindle speed（r/min）	4000、8000、12000、16000
14	optimal machining support mode, cutting parameters are	Feed rate（mm/min）	200、400、600、800
15	selected as variables for cutting deformation experiment.	Cutting depth (mm)	0.02、0.04、0.06、0.08

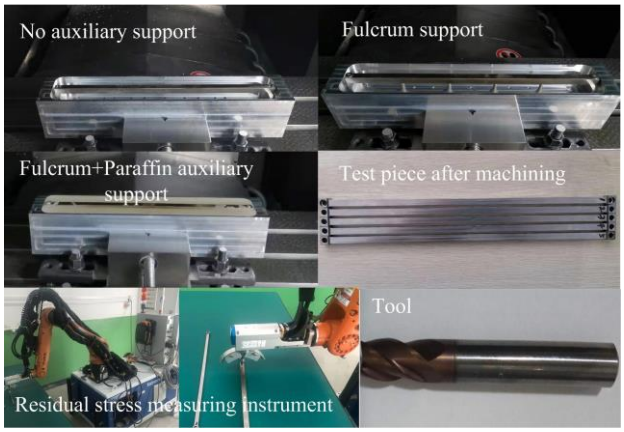

Fig. 6 Experimental Environment of Slender beam Processing

3.3 Influence of processing support mode on deformation of slender beam with weak stiffness

The cutting parameters are n=4000r/min, F=800mm/min, and a_p=0.02mm. At the end of the experiment, the deformation of the workpiece in Z and Y directions was measured online by 3D edge finder. A micrometer was used to measure machining dimension of parts. When measuring the deformation of slender beam, mark the maximum deformation and measure the surface residual stress with residual stress measuring instrument. Table 3 is the experimental data of processing deformation of the slender beam with weak stiffness, and Figure 7 is the influence curve of processing method on the deformation of the slender beam.

Table 3 Processing experimental data of the slender beam with weak stiffness

Serial number	Support mode	Cutting sound	Ridge on top of beam	Beam side pavement	Z-direction deformation (mm)	Y-direction deformation (mm)	Maximum machining deviation (mm)

1	No auxiliary support	Flutter and scream			0.065	0.085	+0.12
2	1 fulcrum to support	Local scream			0.052	0.062	+0.071
3	2 fulcrum to support	Noise			0.043	0.049	+0.045
4	3 fulcrum to support	Small noise			0.037	0.039	-0.039
5	4 fulcrum to support	Normal			0.022	0.028	-0.029
6	Paraffin assisted support	Small noise			0.028	0.031	-0.031
7	1 fulcrum + Paraffin auxiliary support	Normal			0.018	0.021	-0.025
8	2 fulcrum + Paraffin auxiliary support	Normal			0.015	0.016	-0.020
9	3 fulcrum + Paraffin auxiliary support	Normal			0.008	0.012	-0.018
10	4 fulcrum + Paraffin auxiliary support	Normal			0.007	0.010	-0.016

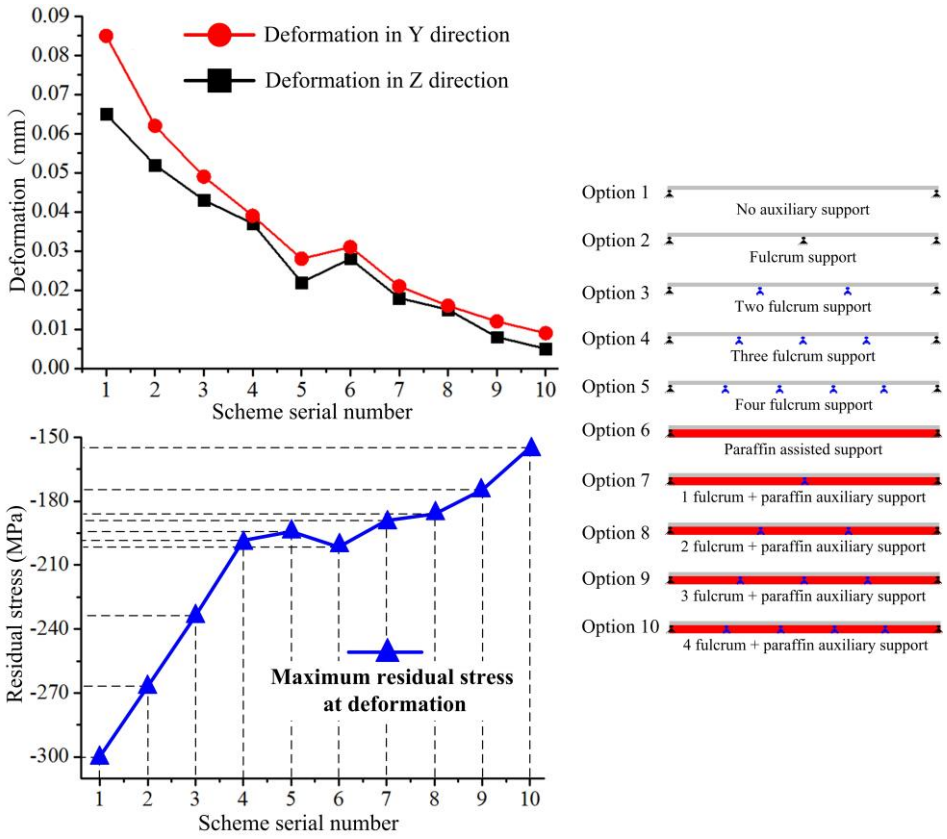

Fig. 7 Influence of processing method on deformation of slender beam

It can be seen in Figure 7 and table 3 that chatter occurred and sharp squeal was produced if the slender beam was machined without auxiliary support, indicating that the chatter was severe during cutting. The reason for the large deviation is that the deformation of slender beams without auxiliary support occurred. From the data table 4, it is observed that as compared to the chatter phenomenon of the slender beam processed without no auxiliary support, this behavior was gradually improved when processing the beam with two-fulcrum auxiliary support, the chatter pattern on the surface was gradually reduced, and the deformation and dimension deviation occurred during machining of the slender beam were gradually improved. Moreover, the residual stress at the maximum deformation becomes smaller after machining. It shows that the unstable chatter phenomenon can be improved and the residual stress is reduced and the machining deformation of slender beam parts can be reduced by upgrading the clamping mode and using the fulcrum support method. When the number of fulcrum was increased to 4, the degree of deformation and machining accuracy of slender beams were controlled within 0.03mm. Although the fulcrum auxiliary support is an effective option to improve the machining accuracy of the slender beam, the combination of fulcrum and paraffin clamping processing can further optimize the machining accuracy. An increase in the number of paraffin and fulcrum provides an opportunity to reduce the deformation and improve the processing accuracy of the slender beam and the residual stress at the maximum deformation of the slender beam after processing is also significantly reduced. When the processing mode was molten material combined with four fulcrums, the dimensional accuracy of beam was 0.016 mm, and the deformation was less than 0.01 mm. From the comparative experiments of 10 clamping methods, it is found that in order to improve the overall processing stiffness and system damping, using the clamping method of the combination of molten

material and fulcrum is a breakthrough to realize the machining of large-scale slender beams.

3.4 Influence of tool wear on machining deformation of slender beam with weak stiffness

The optimal processing support mode was selected from the previous experimental results: four fulcrums + paraffin auxiliary support. The machining experiments of the slender beam with weak stiffness were carried out by using different worn tools. The cutting parameters are n=4000r/min, F=800mm/min, and a_p=0.02mm. At the end of the experiment, the deformation of the workpiece in Z and Y directions was measured online by 3D edge finder. A micrometer was employed to measure machining dimension of parts. Figure 8 shows the curve of machining deformation of slender beam.

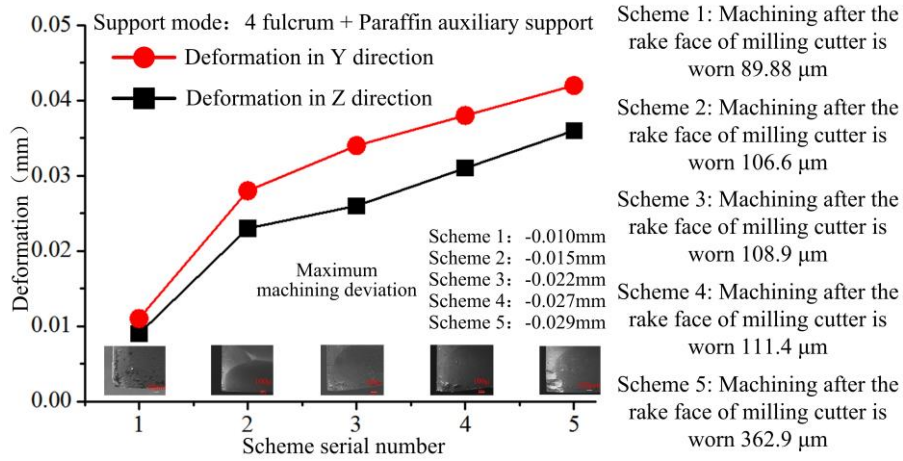

Fig. 8 Influence curve of processing deformation of slender beam

It is seen from the data in Figure 8 that tool wear had a great influence on the machining accuracy of the slender beam. The increasing tool wear caused the machining deformation and dimensional deviation of the slender beam to increase. The deformation and machining accuracy of the slender beam were within 0.05mm. It can also be observed in the Table and the Figure that if the tool wear was effectively controlled, the machining accuracy and deformation of the slender beam could be effectively improved. The reason to achieve such a high-precision processing is that the experimental processing support method improves the overall processing rigidity of the slender beam, and the paraffin also indirectly improves the damping of the processing system and suppresses the chatter phenomenon. Therefore, the experimental results show that under the premise of four fulcrum and molten material processing support mode, the high-precision processing of large-scale slender beam can be effectively realized if the tool wear is effectively controlled, and hence the processing deformation of the slender beam can be reduced.

3.5 Influence of milling parameters on machining deformation of slender beam with weak stiffness

The best processing support mode was selected four fulcrums + paraffin auxiliary support. At the

end of the experiment, the deformation of the workpiece in Z and Y directions was measured online by 3D edge finder. A micrometer was used to measure machining dimension of parts. Figure 9 shows the influence of milling parameters on machining deformation of the slender beam.

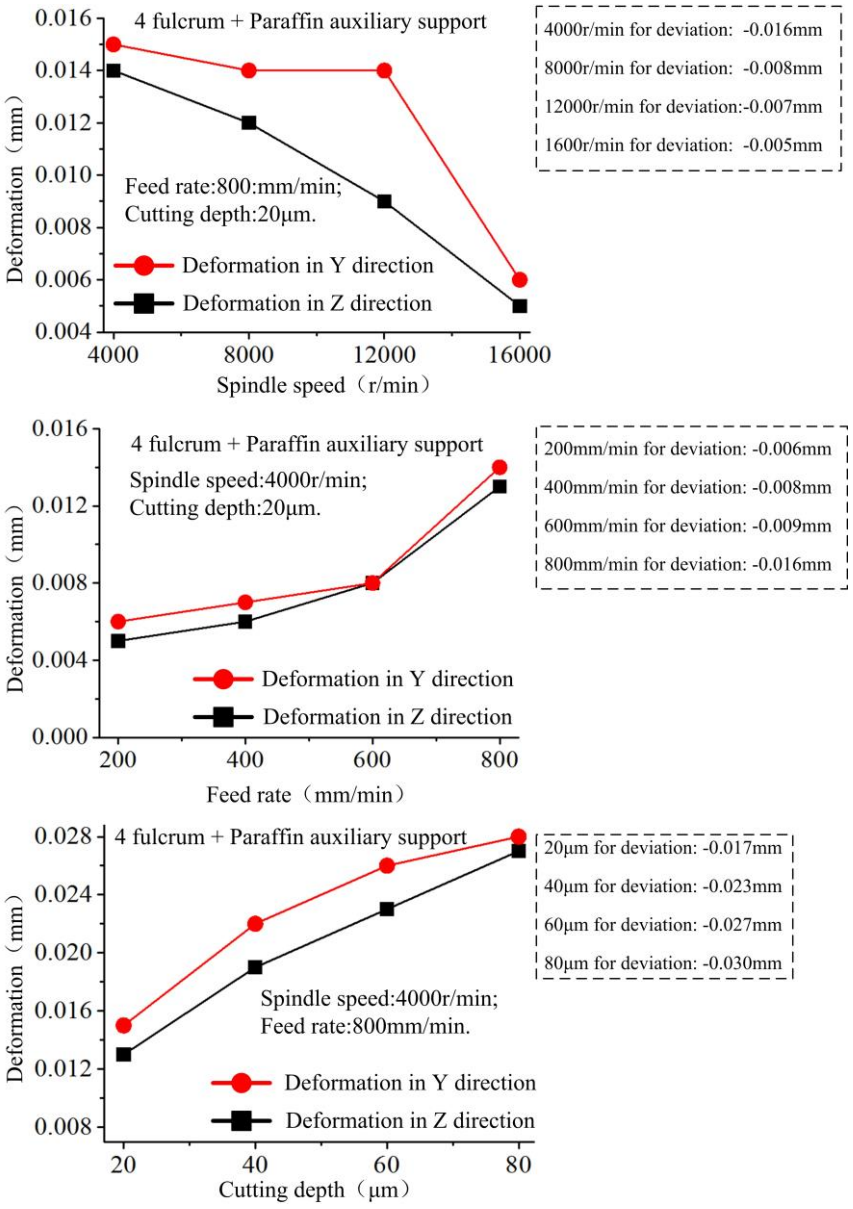

Fig. 9 Influence curve of milling parameters on machining deformation of slender beam

It can be seen in Figure 9 that with the increase of the spindle speed, the machining deformation of the slender beam was gradually reduced, and the machining dimensional accuracy was also gradually improved. However, an increase in feed speed and cutting depth caused the machining dimensional accuracy to become worse. The graph illustrates that the cutting depth has a great impact on the machining deformation of the slender beam while the spindle speed and feed speed have a certain regular influence on the deformation, the change was relatively flat. Although high-speed milling has excellent machining effect on the surface quality of titanium alloy materials, severe tool wear can be

observed when high speed milling of titanium alloy. Therefore, high speed milling is suggested to be used for the finishing process of the slender beam, which not only can effectively control the tool wear, but also improve the machining accuracy of parts.

4 Machining verification of Ti6Al4V typical slender beam with weak stiffness

Figure 10 shows the 3D model of the typical slender beam with weak stiffness to be machined. The model parts are verified by the previous experiments. After the processing, the dimension of the slender beam was measured to evaluate the machining accuracy.

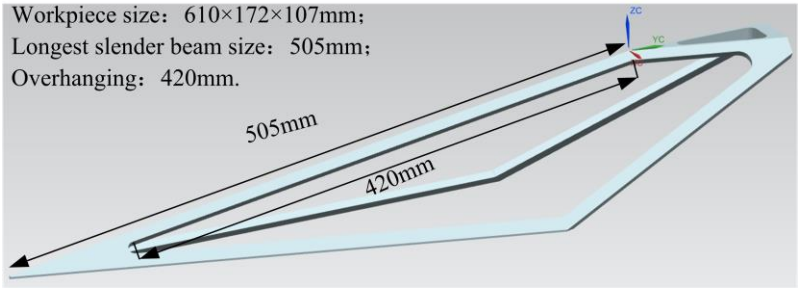

Fig. 10 3D model of typical slender beam with weak stiffness

(1) Milling process of slender beam with weak stiffness

Being similar to the processing of ordinary structural parts, it is necessary to analyze the drawings of the parts and determine the process flow. Figure 11 is the process flow chart.

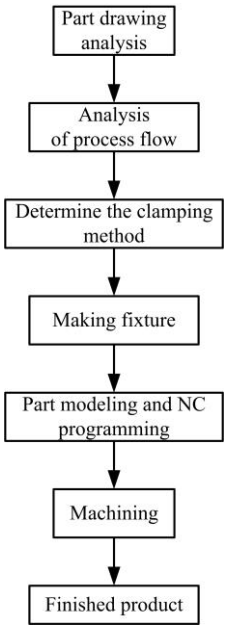

Fig. 11 Process flow chart

(2) Fixture design

According to the clamping experiment of titanium alloy structure parts with weak stiffness, process and fixture design was carried out for typical weak stiffness parts to meet the dimensional accuracy requirements, and repeated clamping operations can be avoided. As shown in Fig. 12, the fixture is provided with a pouring port and an air outlet for pouring liquid materials. The contact surface between the blank and the fixture is bonded with AB glue to avoid external force as much as possible, and reduce the clamping deformation caused by the release of the external force.

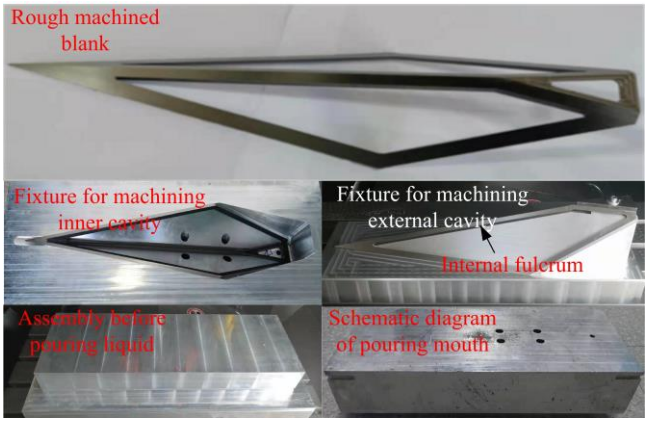

Fig. 12 Large-scale slender beam parts and fixtures

(3) Machining process of the slender beam with weak stiffness

The process is shown in Table 4.

Table 4 Process

Process number	Process name	Cutting parameters	Auxiliary appliances	Equipment
1	Blank parts aging	/	/	Aging furnace
2	The blank parts are clamped on the concave die	/	AB glue, paraffin, custom press pad	/
3	Semi-finish milling inner cavity	n=4000r/min, F=2500mm/min,a_p=0.05mm	Φ6 milling cutter	NC Machining Center
4	Finish milling inner cavity	n=16000r/min, F=800mm/min,a_p=0.02mm	Φ6 milling cutter	NC Machining Center
5	The blank parts are clamped on the convex die	/	AB glue, paraffin, custom press pad	/
6	Semi-finish milling outer contour	n=4000r/min, F=2500mm/min,a_p=0.05mm	Φ6 milling cutter	NC Machining Center
7	Finish milling outer contour	n=16000r/min, F=800mm/min,a_p=0.02mm	Φ6 milling cutter	NC Machining Center
8	Detection	/	3D edge seeker	/
9	Milling windows on both sides	n=16000r/min, F=800mm/min,a_p=0.025mm	Φ6 milling cutter	NC Machining Center
10	Detection	/	3D edge seeker	/

(3) CAM cutting strategy for milling weak stiffness parts

CAM cutting strategy is as follows: the outer profile milling path is from the outer edge to the inner ring milling, and the depth is first. The milling path of the inner cavity is from the inner to the outer edge and the depth is first. The common cutting depth of each tool is constant; the milling tool needs to cut smoothly during machining to make the cutting state stable, and all tool paths of the tool must follow the arc feed path to prevent the deformation of parts due to overcutting. Avoid tool path repetition. Avoid unnecessary damage to workpiece surface caused by cutting tool during machining. The tool path extends a step on the edge to remove the edge burr. The CAM tool feeding strategy is shown in Figure 13 below.

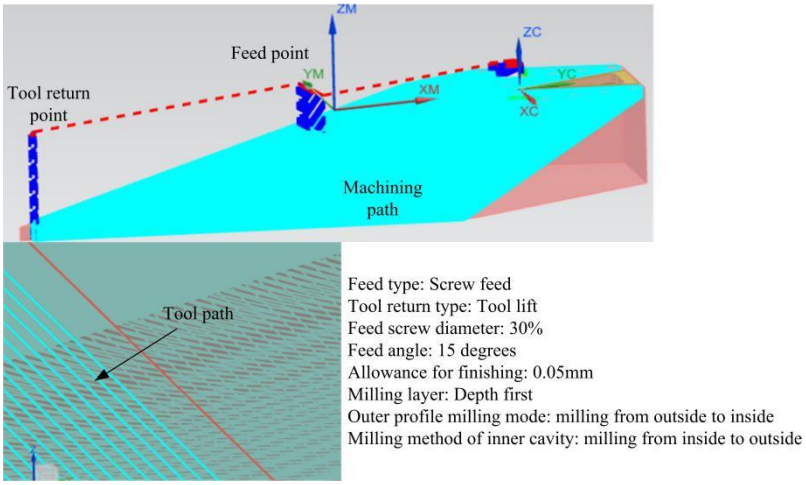

Fig. 13 CAM cutting strategy

As shown in Figure 14, the surface quality of the processed weak rigid parts is in good condition, the maximum deformation of the longest slender beam in the middle is 0.019mm, the size deviation of the 420mm×8.6mm×8.6mm slender beam in the middle is -0.017mm, the machined surface is bright, and the roughness is less than 0.5μm.

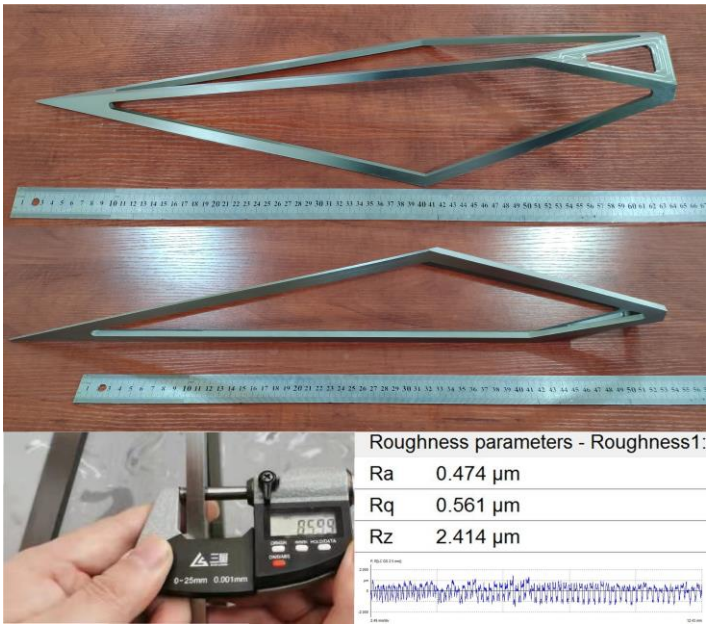

Fig. 14 Parts drawing of titanium alloy with weak stiffness

5 Conclusions

Aiming at the deformation problem of large-scale slender beam with weak stiffness, this paper has

carried out theoretical analysis on milling stability, and has performed experiments by adopting some methods to restrain the deformation. In the end, the processing of typical large-scale parts with weak stiffness was verified. The conclusions are as follows:

(1) From the theoretical analysis, it can be concluded that improving cutting stability can be achieved by increasing the damping, improving the overall stiffness of the processing system, and reducing the cutting force so as to effectively achieve high-precision processing of parts.

(2) When processing the slender beam parts, the fulcrum and paraffin combined with auxiliary support is an optimal way to increase the overall system damping, improve the overall stiffness of the processing system, and suppress the processing chatter effect. This method is capable of greatly improving the accuracy and efficiency during processing of slender beam parts.

(3) Under the premise of fulcrum and paraffin combined with auxiliary support method, if the tool wear is effectively controlled, the high-precision machining of large-scale slender beam can be effectively realized, and the machining deformation of the slender beam can be reduced.

(4) Although high-speed milling has excellent machining effect on the surface quality of titanium alloy materials, severe tool wear is observed in the process of high-speed milling of the titanium alloy. Therefore, high speed milling is recommended for the finishing process of the slender beam, which not only can effectively control the tool wear, but also improve the machining accuracy of parts.

(5) Through the theoretical and technical support of the experimental scheme, the machining of typical large-scale slender beams with weak stiffness can be realized.

Author contribution The authors discussed each reference paper together and contributed useful ideas for this manuscript. The authors sincerely thank Professor Hua-dong Yu of Changchun University of Science and Technology for his critical discussion and reading during manuscript preparation.

Funding This work was supported by "Supported by national basic scientific research program" (JCKY2017208B006) and "Stability support project"(WDZC2019JJ016).

Availability of data and material Not applicable

Code availability Not applicable

Declarations

Competing interests The authors declare no competing interests.

Consent to participate The authors consent to participate.

Consent to publish Yes

References

1. Lei Yuan (2016) Surface Quality Analysis and Machining Process Parameters Optimization of Thin-Walled Workpiece in Milling[D]. Wuhan University of Technology (in Chinese)

2. WEi Zhang (2011) Surface Integrity and Deformation Forecasting in High Speed Cutting Titanium Alloy Thin-walled Component[D]. Harbin University of science and technology(in Chinese)

3. Ervis (2005) A mathematical model for the estimation of effects of residual Stresses in aluminum parts[D]. Washington University

4. Keith A Y (2005) Machining induced residual stress and distortion of thin-parts[D]. Washington University

5. Ratchev S, Huang W, Liu S (2004) Modeling and simulation environment for machining of low-rigidity components[J] Journal of Materials Processing Technology 153(12)：67-73

6. Ratchev S，Liu S，Huang W (2006) An advanced FEA based force induced error compensation strategy in milling[J]. Intemational Journal of Machine Tools and Manufacture 46(5):542-551

7. Ratchev S，Liu S，Beeker A A (2005) Error compensation strategy in milling flexible thin wall parts[J]. Journal of Materials Processing Technology 162:673-681

8. Tlusty J, Smith S, Badrawy J (1997) Design of a high speed machine for aluminum aircraft parts[J]. Manufacturing Science and Technology 2:253-259

9. Hiroyasu I (1997) High accurate machining ofthin wall shape work piece by end mill[C]. Japanese Mechanical institute Conference Proceeding 63:605-610

10.Yunlin Huang (2015) Study on the stability and quality of thin-walled workpiece in high-speed milling[D]. Nanjing University of Technology(in Chinese) ·

11. Ming Wang (2015) Research on processing mechanism of rotary ultrasonic machining of SiCp/Al composites and processing stability of thin-walled workpiece[D]. Harbin Institute of Technology(in Chinese) ·

12. Dong G, Wang X, Gao S (2018) Molecular dynamics simulation and experiment research of cutting-tool wear mechanism for cutting aluminum alloy[J], International Journal of Advanced Manufacturing Technology 96(1-4), 1123-1137

13. Jiapeng Lu (2016) Study on the burr formation mechanism and sizes prediction theory in cutting metal materials[D]. Hunan University(in Chinese) ·

14. Liu J L, Zhang B, Bai Q (2018) Temperature prediction of tool/workpiece contact zone in titanium milling [J].

Acta Aero-nautica et Astronautica Sinica 39(12): (in Chinese)

15. Xiaohui Zhang (2015) Investigation on the mechanism of the residual stress and control method of machining accuracy for the complex thin-walled parts[D]. Donghua University(in Chinese)

16. HUANG Qianyou，NIU Xinghua，ZHAO Tiemin，ZHENG Yingjie，DONG Houfu (2017) Calculation and simulation of chatter stability for milling based on MATLAB[J]. JOURNAL OF TIANJIN UNIVERSITY OF TECHNOLOGY (33) (in Chinese)

17. LI Zhong-qun, LIU Qiang (2007) An simulation algorithm of chatter stability lobes for milling and its implementation based on MATLAB[J]. Machinery Design & Manufacture (7):109-112 (in Chinese)

18. Qingqing Wang, Zhanqiang Liu (2016) Evolutions of grain size and micro-hardness during chip formation and machined surface generation for Ti-6Al-4V in high-speed machining[J]. Int J Adv Manuf Technol 82:1725–1736

19. Ning Hou, Minghai Wang, Yong Zhang, Hao Wang, Ce Song (2021) Insights into the fatigue property of titanium alloy Ti-6Al-4V in aero-engine from the subsurface damages induced by milling: state of the art[J]. Int J Adv Manuf Technol 113:1229–1235

Figures

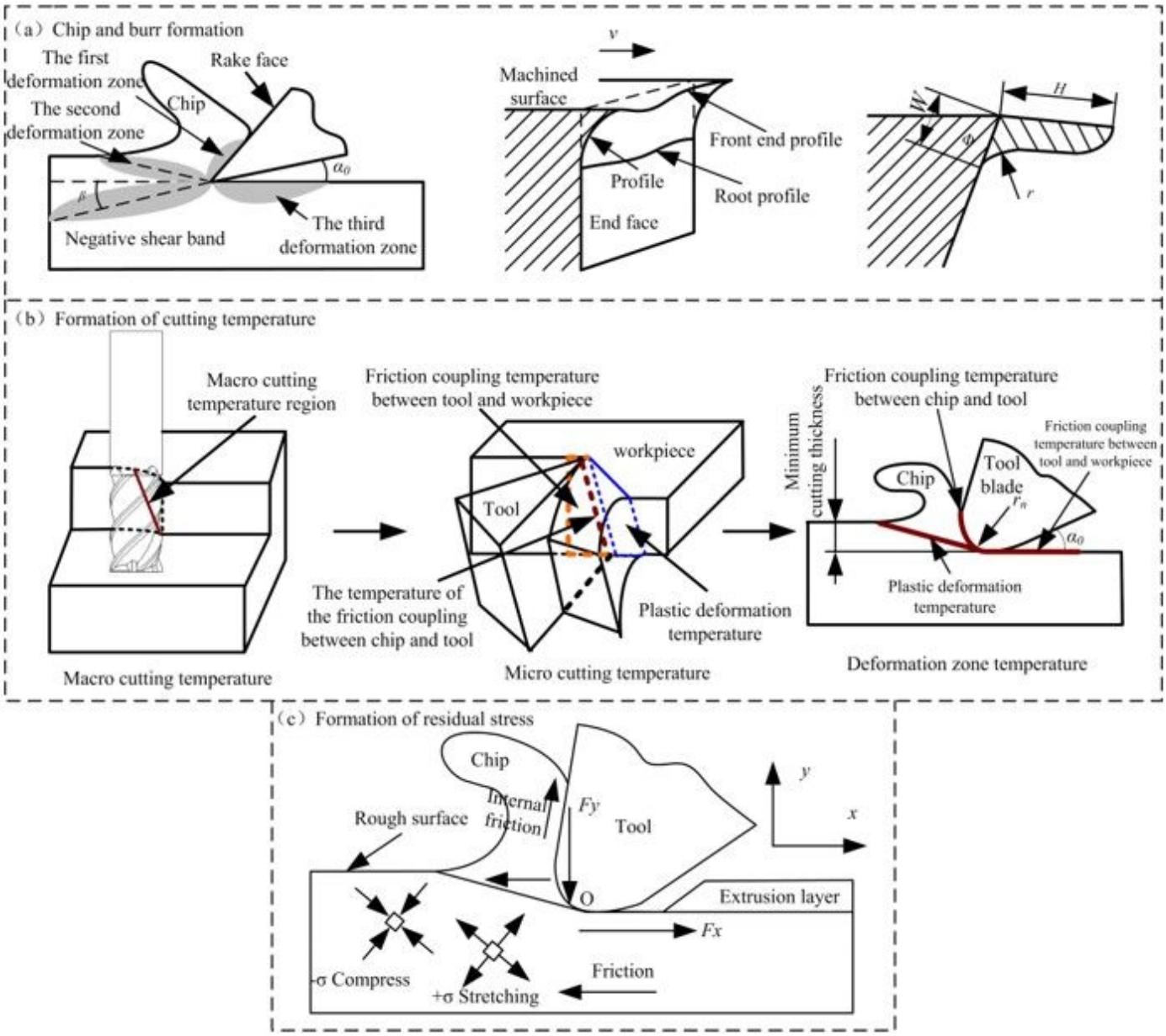

Figure 1

Principle of Metal Cutting

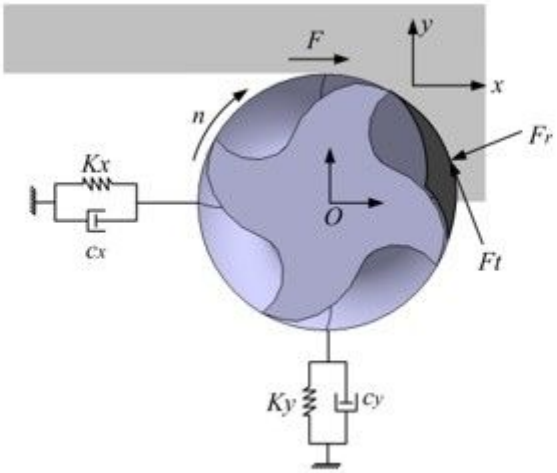

Figure 2

Milling Vibration Systems

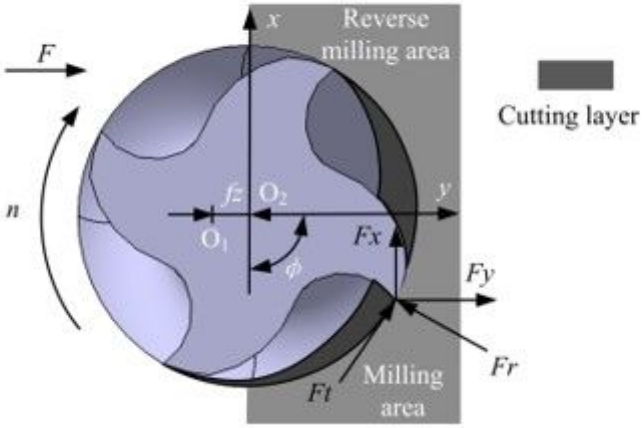

Figure 3

Force distribution of milling cutter

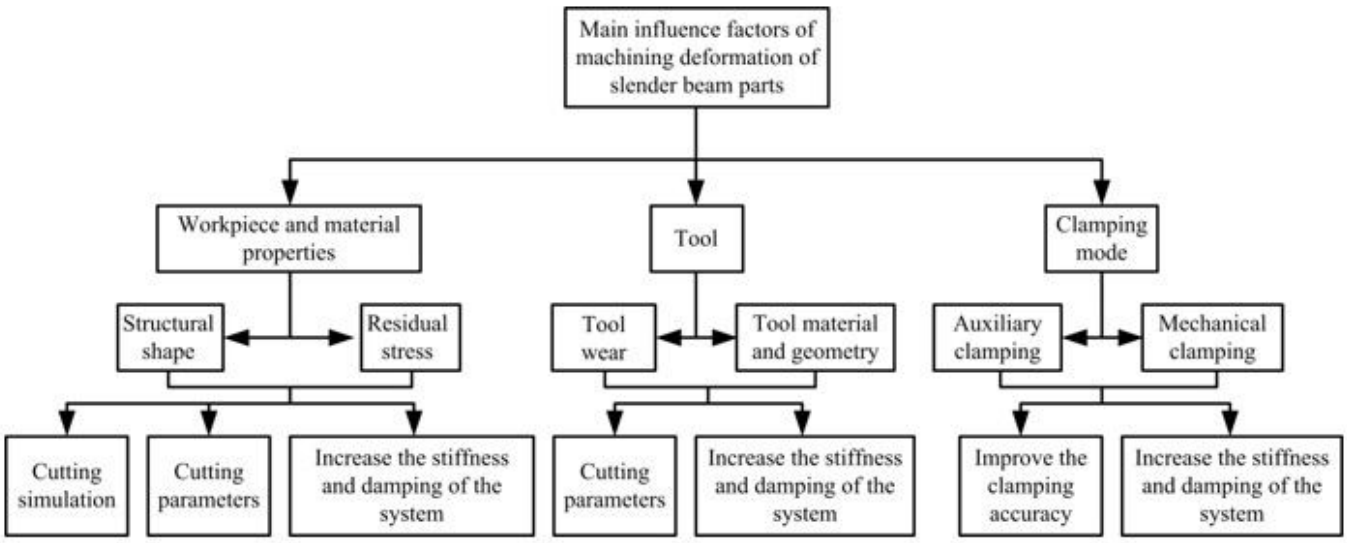

Figure 4

Influence factors of deformation of slender beam parts with weak stiffness

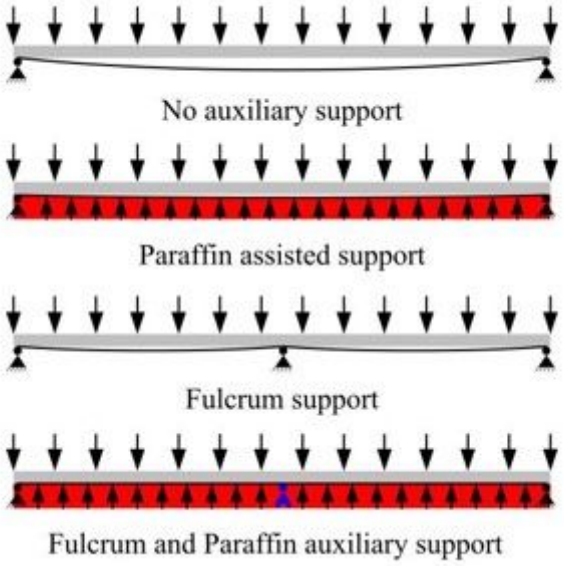

Figure 5

Schematic illustration of deformation effect of auxiliary support

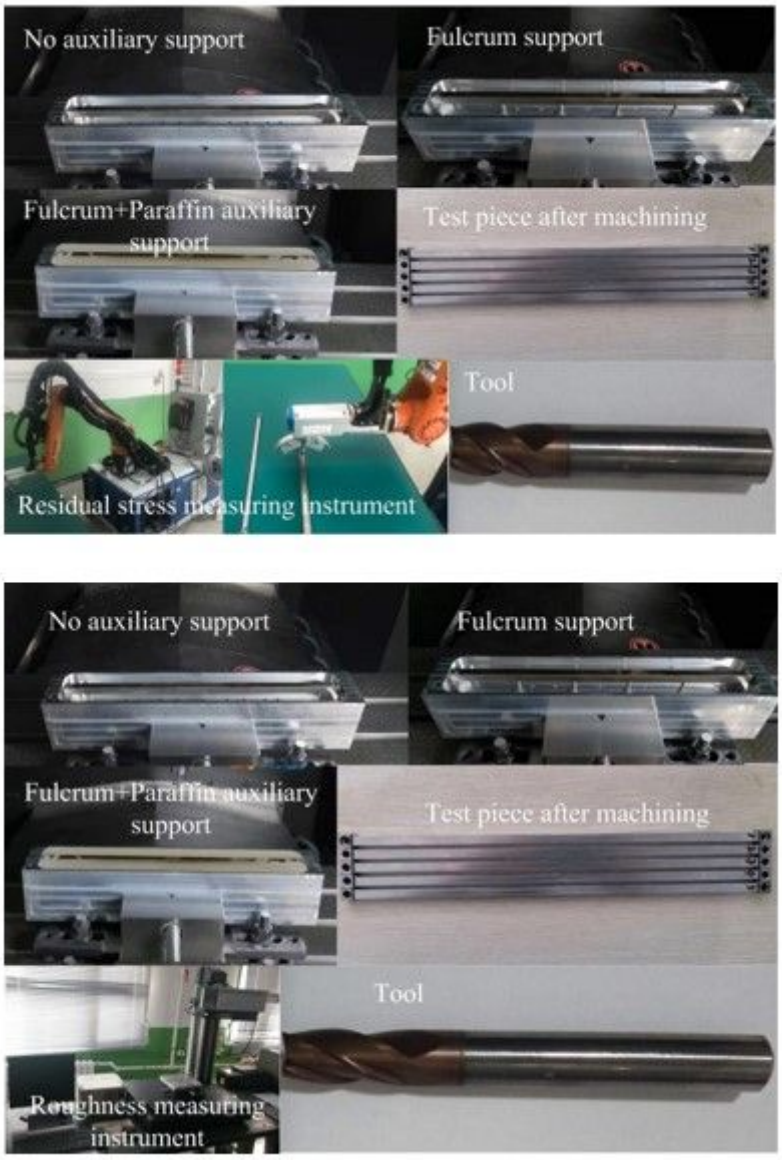

Figure 6

Experimental of Slender beam Processing

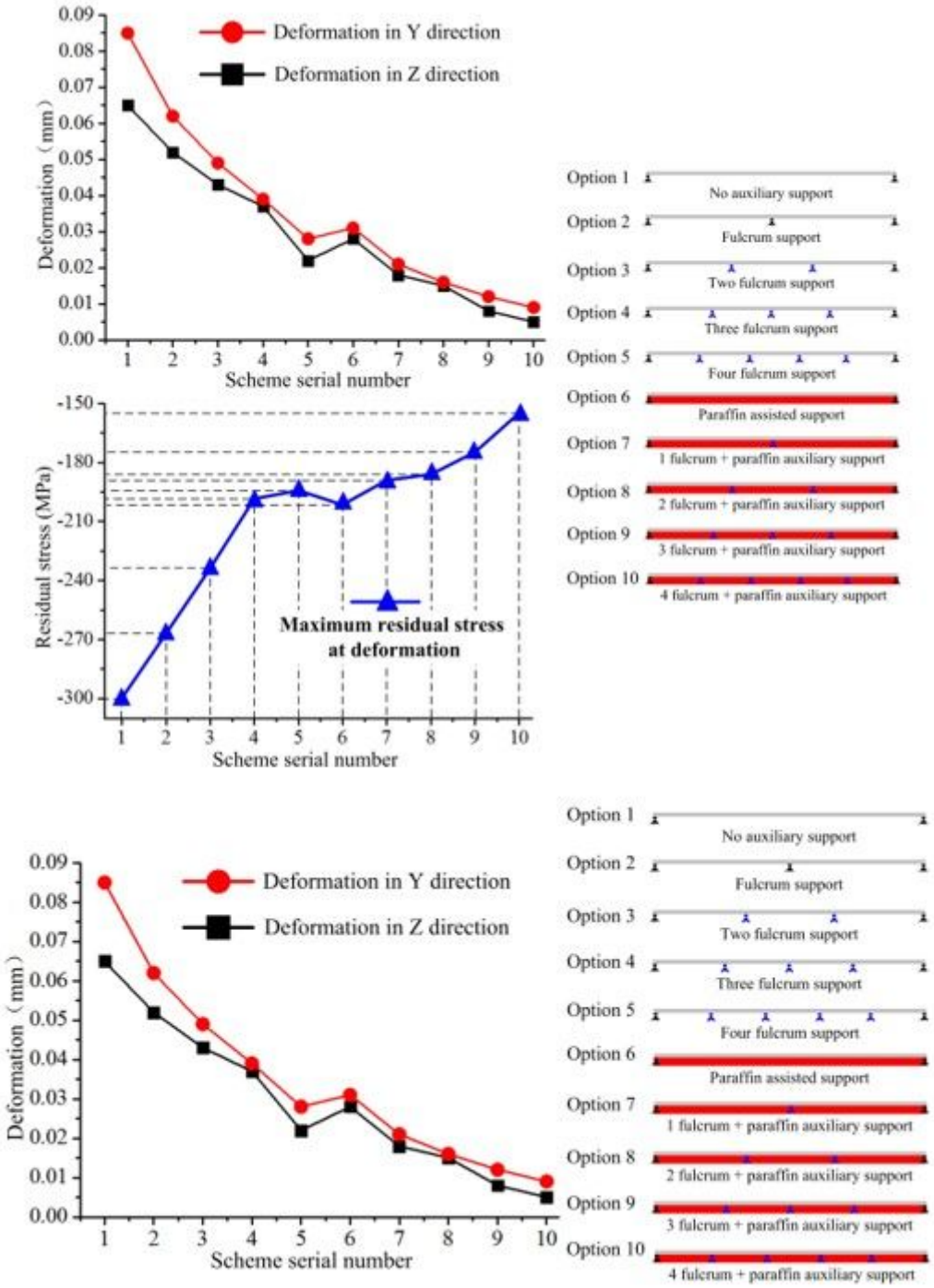

Figure 7

Influence of processing method on deformation of slender beam

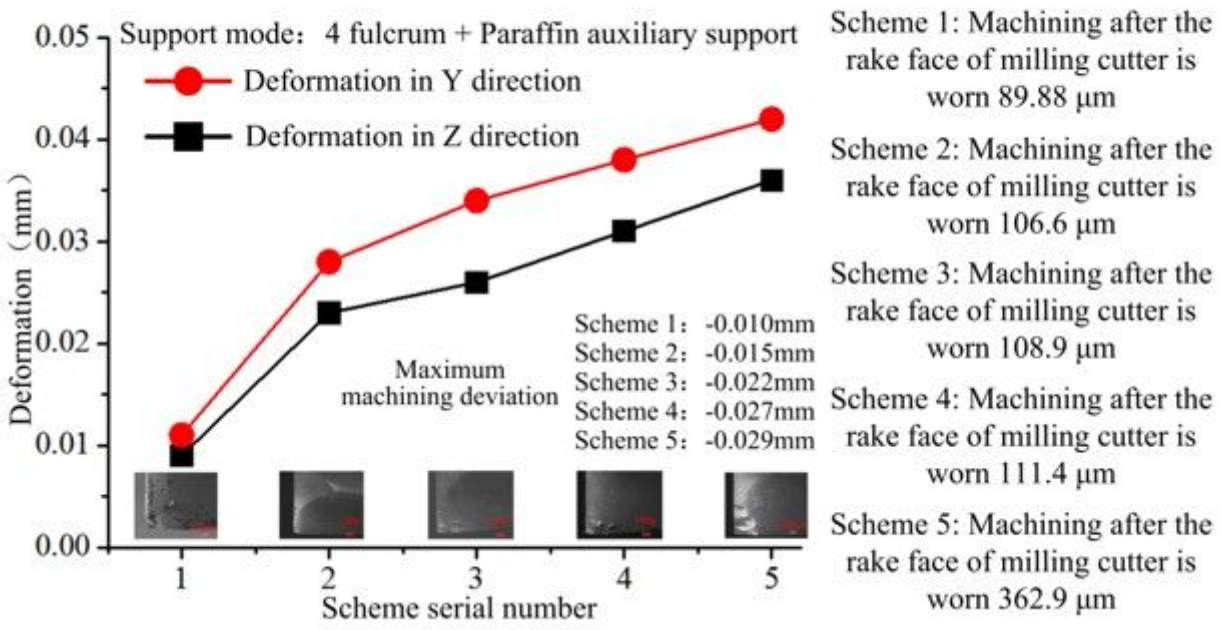

Figure 8

Influence curve of processing deformation of slender beam

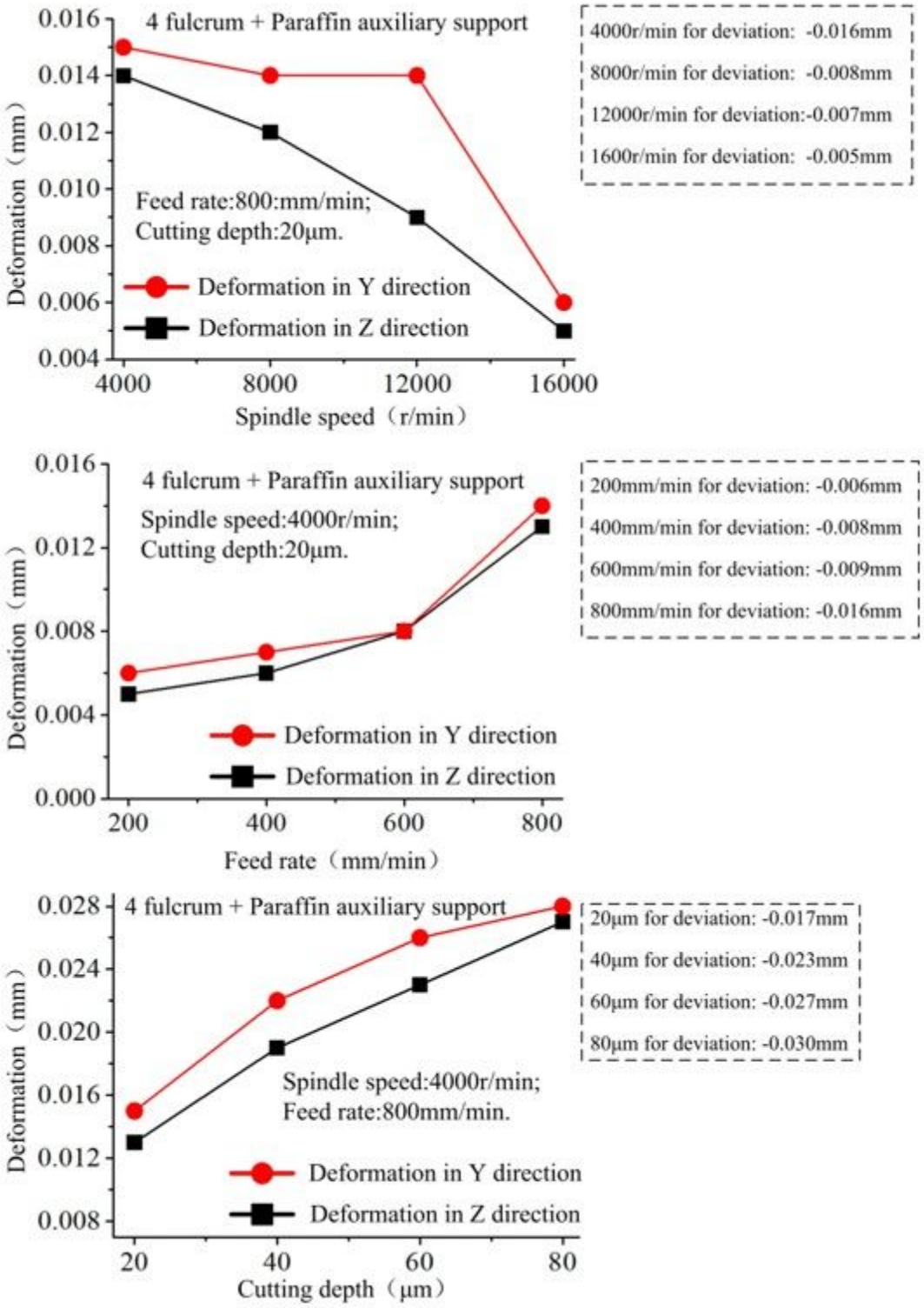

Figure 9

Influence curve of milling parameters on machining deformation of slender beam

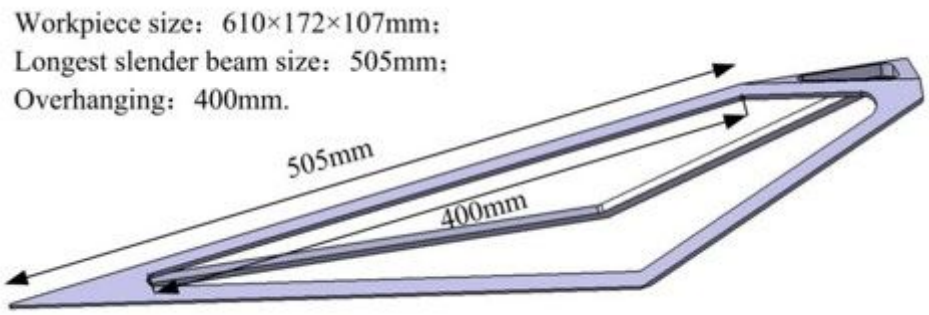

Figure 10

3D model of typical slender beam with weak stiffness

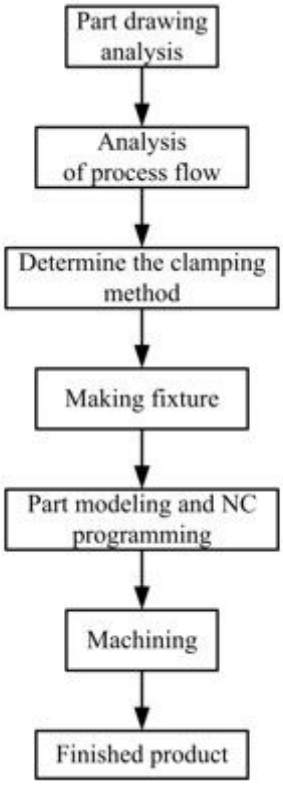

Figure 11

Process flow chart

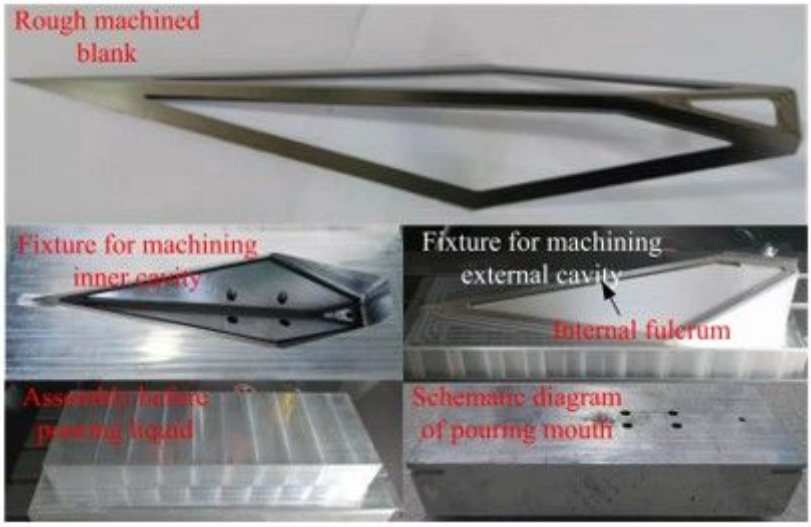

Figure 12

Large scale slender beam parts and Fixtures

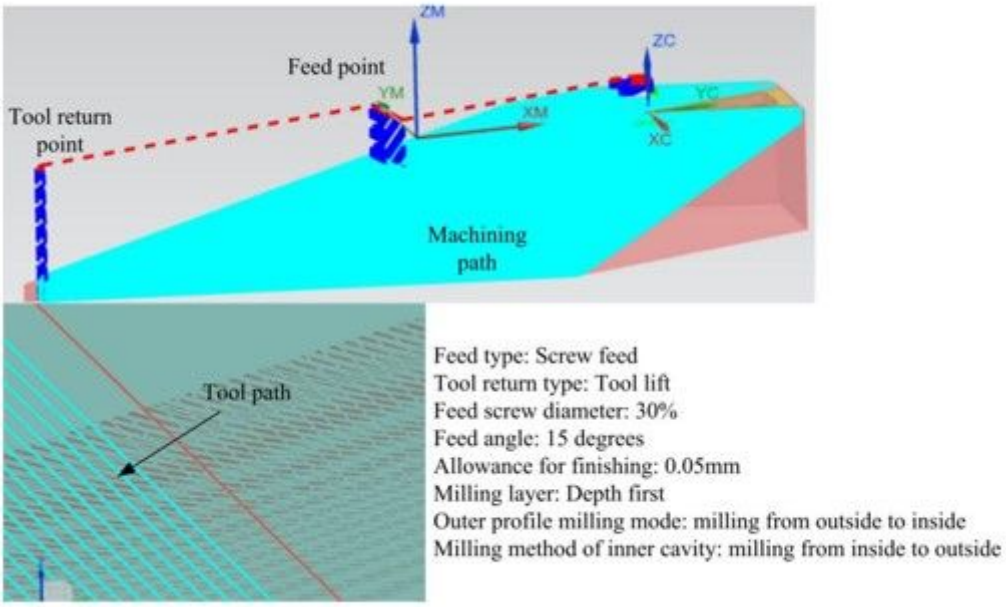

Figure 13

CAM cutting strategy

Figure 14

Parts drawing of titanium alloy with weak stiffness